Article

Dipolar Waves Map the Structure and Topology of Helices in Membrane Proteins

Michael F. Mesleh, Sangwon Lee, Gianluigi Veglia, David S. Thiriot, Francesca M. Marassi, and Stanley J. Opella

J. Am. Chem. Soc., **2003**, 125 (29), 8928-8935• DOI: 10.1021/ja034211q • Publication Date (Web): 25 June 2003

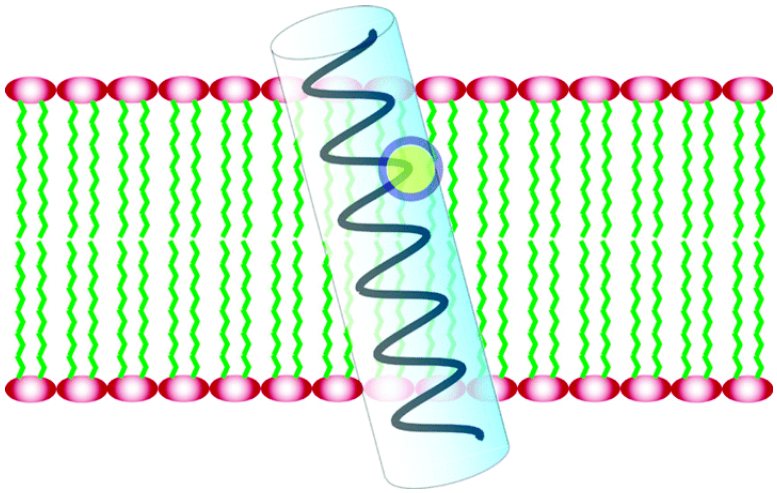

J|A|C|S
ARTICLES
Published on Web 06/25/2003

Dipolar Waves Map the Structure and Topology of Helices in Membrane Proteins

Michael F. Mesleh,[†] Sangwon Lee,[†] Gianluigi Veglia,[‡] David S. Thiriot,[†] Francesca M. Marassi,[§] and Stanley J. Opella*,[†]

Contribution from the Department of Chemistry and Biochemistry, University of California, San Diego, 9500 Gilman Drive La Jolla, California 92093, Department of Chemistry, University of Minnesota, Minneapolis, 207 Pleasant Street, Minnesota 53485, and The Burnham Institute, 10901 North Torrey Pines Road, La Jolla, California 92037

Received January 16, 2003; E-mail: sopella@ucsd.edu

Abstract: Dipolar waves describe the structure and topology of helices in membrane proteins. The fit of sinusoids with the 3.6 residues per turn period of ideal α-helices to experimental measurements of dipolar couplings as a function of residue number makes it possible to simultaneously identify the residues in the helices, detect kinks or curvature in the helices, and determine the absolute rotations and orientations of helices in completely aligned bilayer samples and relative rotations and orientations of helices in a common molecular frame in weakly aligned micelle samples. Since as much as 80% of the structured residues in a membrane protein are in helices, the analysis of dipolar waves provides a significant step toward structure determination of helical membrane proteins by NMR spectroscopy.

Introduction

Helical membrane proteins are ideal candidates for analysis with dipolar waves.[1,2] Like PISA (polarity index slant angle) Wheels,[3,4] from which they are derived, dipolar waves are a representation of the mapping of protein structure onto NMR spectra through the anisotropic nuclear spin interactions in aligned samples. Sinusoidal oscillations of chemical shift[5] and dipolar coupling[1,2] frequencies have been analyzed for helical residues in membrane proteins. As much as 80% of the structured residues of membrane proteins are in helices. Not only is little or no other regular secondary structure present in the turns, loops, and terminal regions but also substantial internal motions affect many of the nonhelical residues. As a result, identifying and characterizing the relative rotations and orientations of the helices in proteins and their global orientations in the bilayer go a long ways toward determining the three-dimensional structures and topologies of membrane proteins.

Previous structural studies of helical membrane proteins focused on the topology of their helices by using chemical modifications as a probe,[6,7] diffraction experiments,[8,9] electron microscopy,[10] and magnetic resonance experiments, including some that make use of the 3.6 residues per turn periodicity of α-helices.[11,12] Recent X-ray diffraction structures of relatively small channel-forming proteins provide considerable detail about the properties of helices in membrane proteins.[13−17]

In this article, applications of dipolar waves to membrane proteins are illustrated using examples of 20−80 residue polypeptides with representative transmembrane and in-plane helices. Since many membrane proteins appear to be assembled from modules of these structural elements, this approach may be scalable to substantially larger membrane proteins. The experimental results enable comparisons to be made between the same residues in polypeptides corresponding to individual helical domains and full-length proteins to address the influence of protein context and in micelle and bilayer samples to address the influence of lipid context on their structural properties. The relatively large amounts of membrane-associated polypeptides required for NMR studies can be prepared by expression in bacteria, which offers opportunities for uniform ^{15}N labeling

[†] University of California, San Diego.
[‡] University of Minnesota.
[§] The Burnham Institute.

(1) Mesleh, M. F.; Veglia, G.; DeSilva, T. M.; Marassi, F. M.; Opella, S. J. *J. Am. Chem. Soc.* **2002**, *124*, 4206−4207.
(2) Mesleh, M. F.; Opella, S. J. *J. Magn. Reson.*, in press.
(3) Marassi, F. M.; Opella, S. J. *J. Magn. Reson.* **2000**, *144*, 150−155.
(4) Wang, J.; Denny, J.; Tian, C.; Kim, S.; Mo, Y.; Kovacs, Z.; Song, Z.; Nishimura, K.; Gan, Z.; Fu, R.; Quine, J. R.; Cross, T. A. *J. Magn. Reson.* **2000**, *144*, 162−167.
(5) Kovacs, F. A.; Denny, J. K.; Song, Z.; Quine, J. R.; Cross, T. A. *J. Mol. Biol.* **2000**, *295*, 117−125.
(6) Arkin, I. T.; MacKenzie, K. R.; Fisher, L.; Aimoto, S.; Engelman, D. M.; Smith, S. O. *Nat. Struct. Biol.* **1996**, *3*, 240−243.
(7) Nagy, J. K.; Lau, F. W.; Bowie, J. U.; Sanders, C. R. *Biochemistry* **2000**, *39*, 4154−4164.
(8) Trewhella, J.; Popot, J. L.; Zaccai, G.; Engelman, D. M. *EMBO J.* **1986**, *5*, 3045−3049.
(9) Luecke, H.; Schobert, B.; Richter, H. T.; Cartailler, J. P.; Lanyi, J. K. *J. Mol. Biol.* **1999**, *291*, 899−911.
(10) Unwin, N. *Nature* **1995**, *6509*, 37−43.
(11) Altenbach, C.; Marti, T.; Khorana, H. G.; Hubbell, W. L. *Science* **1990**, *248*, 1088−1092.
(12) Luchette, P. A.; Prosser, R. S.; Sanders, C. R. *J. Am. Chem. Soc.* **2002**, *124*, 1778−1781.
(13) Doyle, D. A.; Cabral, J. M.; Pfuetzer, R. A.; Kuo, A.; Gulbis, J. M.; Cohen, S. L.; Chait, B. T.; MacKinnon, R. *Science* **1998**, *280*, 69−73.
(14) Zhou, Y.; Morais-Cabral, J. H.; Kaufman, A.; MacKinnon, R. *Nature* **2001**, *414*, 43−53.
(15) Spencer, R. H.; Rees, D. C. *Annu. Rev. Biophys. Biomol. Struct.* **2002**, *31*, 207−233.
(16) Fu, D.; Libson, A.; Miercke, L. J.; Weitzman, C.; Nollert, P.; Krucinski, J.; Stroud, R. M. *Science* **2000**, *290*, 481−486.
(17) Murata, K.; Mitsuoka, K.; Hirai, T.; Walz, T.; Agre, P.; Heymann, J. B.; Engel, A.; Fujiyoshi, Y. *Nature* **2000**, *407*, 599−605.

10.1021/ja034211q CCC: $25.00

of the backbone.[18] Membrane-associated polypeptides can be expressed as inclusion body-forming fusion proteins and then isolated, purified, and reconstituted with lipids that self-assemble to form micelles, bicelles, or bilayers.[19] With careful sample preparation, it is possible to obtain well-resolved NMR spectra of membrane proteins in all three types of samples using a combination of solution NMR and solid-state NMR instruments and methods.[20] A few reports on solution NMR of proteins with multiple transmembrane helices have described spectral complexities in the form of missing, doubled, and broadened resonances due to the variable effects of internal dynamics of loop regions as well as the transmembrane helices themselves.[21−23] Although high-quality solution NMR spectra have been obtained for some moderately large membrane proteins,[20,24,25] there are only a few examples where it has been possible to resolve and assign a sufficient number of "long-range" NOEs to determine protein folds that include the helices.[26−28] However, this limitation is largely overcome by the preparation of weakly aligned micelle samples[29−31] for the measurement of residual dipolar couplings (RDCs)[32] with solution NMR experiments and the preparation of completely aligned bilayer samples for the measurement of unaveraged dipolar couplings[33] with solid-state NMR experiments. The three-dimensional structures of several membrane peptides and proteins have been determined by solid-state NMR spectroscopy.[34−36]

Dipolar waves provide direct and rapid access to the dominant features of helical membrane proteins. This is a result of the fact that the periodicity of α-helices is mapped onto NMR spectra in a straightforward manner by the anisotropy of dipolar couplings. The fit of the magnitudes of the $^1H-^{15}N$ dipolar couplings from the backbone amide sites of the polypeptides as a function of residue number to sinusoids of periodicity 3.6 can be used to characterize the lengths, deformations, orientations, and rotations of hydrophobic and amphipathic α-helices in both bilayer and micelle environments.[2] While characterization of the lengths and deformations of helices can be accomplished without an explicit determination of the overall orientation of the molecule, solid-state NMR experiments on completely aligned samples enable the determination of the absolute orientation within the bilayer and, hence, the overall topology of the protein.

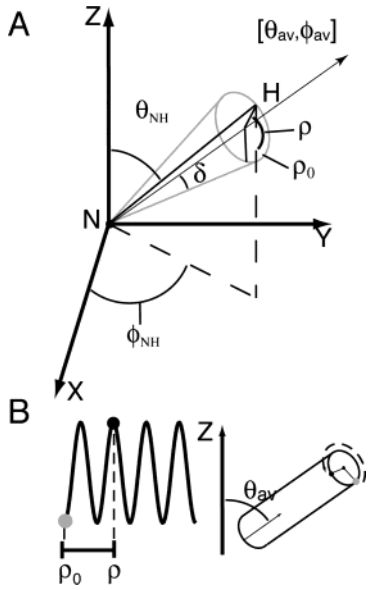

Figure 1. (A) The NH bond vectors (θ_{NH} and ϕ_{NH}) in an α-helix are distributed on a cone tilted at an angle δ away from the helix axis (θ_{av} and ϕ_{av}) which has a given orientation in the frame that describes the molecular alignment and averaging. (B) This results in sinusoidal oscillations in which the location of a particular experimental measurement along the sinusoid determined the rotation of that residue about the helix axis.

Experimental Methods

Sample Preparation. All of the polypeptides were expressed in *E. coli* grown in minimal media with $(^{15}NH_4)_2SO_4$ as the sole nitrogen source. The expression, isolation, purification, and preparation of completely aligned bilayer samples of the 25-residue acetylcholine M2 peptide[35] and the 50-residue fd coat protein[33] (Y21M mutant) have been described. The 20-residue peptide corresponding to the N-terminal amphipathic helix of the fd coat protein (fd^N) was expressed with a KetoSteroid Isomerase/His tag fusion as multiple tandem copies in the pET31 expression vector (Novagen, Madison, WI) in BLR(DE3) pLysS cells (Novagen, Madison, WI). The fusion protein was isolated on Ni^{2+} resin, cleaved with cyanogen bromide, and purified by ultrafiltration followed by HPLC. MerF was expressed as a fusion with an N-terminal His-tag and a Trp leader peptide as previously described for another membrane protein of the same size[37] using the Trp-ΔLE plasmid in BL21(DE3) PlysS cells. Following isolation and cleavage of the fusion protein, final purification of the 80-residue MerF polypeptide was accomplished using size-exclusion chromatography.

Completely aligned lipid bilayers were formed by depositing lipid/protein mixtures onto thin glass slides, which were then dehydrated and rehydrated by incubation in a sealed chamber with 94% relative humidity at 42 °C. Solution NMR samples of the fd coat protein and the fd^N peptide were made with 1 mM ^{15}N-labeled protein in 500 mM SDS, 40 mM NaCl at pH 4.0. Samples of the 80-residue MerF protein were made in 600 mM SDS, 20 mM PO_4 buffer, and 40 mM DTT at pH 6.5. The samples of the fd coat protein and the fd^N peptide in micelles were weakly aligned in a 7% polyacrylamide gel by soaking

(18) Cross, T. A.; DiVerdi, J. A.; Opella, S. J. *J. Am. Chem. Soc.* **1982**, *104*, 1759−1761.
(19) Opella, S. J.; Ma, C.; Marassi, F. M. *Methods Enzymol.* **2001**, *280*, 285−313.
(20) Opella, S. J. *Nat. Struct. Biol. NMR Suppl.* **1997**, *280*, 845−848.
(21) Schwaiger, M.; Lebendiker, M.; Yerushalmi, H.; Coles, M.; Groger, A.; Schwartz, C.; Schuldiner, S.; Kessler, H. *Eur. J. Biochem.* **1998**, *254*, 610−619.
(22) Klein-Seetharaman, J.; Reeves, P. J.; Loewen, M. C.; Getmanova, E. V.; Chung, J.; Schwalbe, H.; Wright, P. E.; Khorana, H. G. *Proc. Natl. Acad. Sci. U.S.A.* **2002**, *99*, 3452−3457.
(23) Schubert, M.; Kolbe, M.; Kessler, B.; Oesterhelt, D.; Schmieder, P. *ChemBioChem* **2002**, *3*, 1019−1023.
(24) Oxenoid, K.; Sonnichsen, F. D.; Sanders, C. R. *Biochemistry* **2001**, *40*, 5111−5118.
(25) Okon, M.; Frank, P. G.; Yves, M. L.; Cushley, R. *FEBS Lett.* **2001**, *487*, 390−396.
(26) Almeida, F. C.; Opella, S. J. *J. Mol. Biol.* **1997**, *270*, 481−495.
(27) MacKenzie, K. R.; Prestegard, J. H.; Engelman, D. M. *Science* **1997**, *276*, 131−133.
(28) Girvin, M. E.; Rastogi, V. K.; Abildgaard, F.; Markley, J. L.; Fillingame, R. H. *Biochemistry* **1998**, *37*, 8817−8824.
(29) Ma, C.; Opella, S. J. *J. Magn. Reson.* **2000**, *146*, 381−384.
(30) Veglia, G.; Opella, S. J. *J. Am. Chem. Soc.* **2000**, *47*, 11753−11754.
(31) (a) Sass, H. J.; Musco, G.; Stahl, S. J.; Wingfield, P. T.; Grzesiek, S. *J. Biomol. NMR* **2000**, *18*, 303−309. (b) Ishii, Y.; Markus, M. A.; Tycko, R. *J. Biomol. NMR* **2001**, *21*, 141−151. (c) Chou, J. J.; Gaemers, S.; Howder, B.; Louis, J. M.; Bax, A. *J. Biomol. NMR* **2001**, *21*, 377−382.
(32) (a) Prestegard, J. H.; Al-Hashimi, H. M.; Tolman, J. R. *Q. Rev. Biophys.* **2000**, *33*, 371−424. (b) Bax, A.; Kontaxis, G.; Tjandra, N. *J. Biomol. NMR* **2001**, *21*, 377−382.
(33) Marassi, F. M.; Ramamoorthy, A.; Opella, S. J. *Proc. Natl. Acad. Sci. U.S.A.* **1997**, *94*, 8551−8556.
(34) Ketchem, R. R.; Kim, S.; Kovacs, F.; Cross, T. A. *Science* **1993**, *261*, 1457−1460.
(35) Opella, S. J.; Marassi, F. M.; Gesell, J. J.; Valente, A. P.; Kim, Y.; Oblatt-Montal, M.; Montal, M. *Nat. Struct. Biol.* **1999**, *6*, 374−379.
(36) Wang, J.; Kim, S.; Kovacs, F.; Cross, T. A. *Protein Sci.* **2001**, *10*, 2241−2250.
(37) Ma, C.; Marassi, F. M.; Jones, D. H.; Straus, S. K.; Bour, S.; Strebel, K.; Schubert, U.; Oblatt-Montal, M.; Montal, M, Opella, S. J. *Protein Sci.* **2002**, *11*, 546−557.

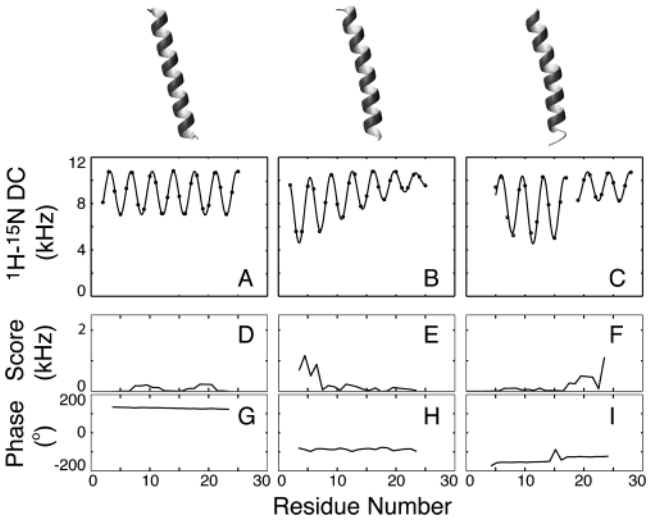

Figure 2. ^{1}H−^{15}N dipolar couplings are simulated for (A) a straight ideal α-helix, (B) an α-helix with a 55 Å radius of curvature, and (C) an ideal α-helix with a 20° kink with their average axis tilted 15° relative to the alignment *z*-axis. (D, E, F) The average error per point shows that the periodicity in all cases is 3.6 except near the ends where this periodicity is disrupted. (G, H, I) The phase is also diagnostic, where the kink is evidenced by a slight change in the phase of one sinusoid relative to the other.

the protein solution into the gel and limiting the length of expansion in the NMR sample tube to induce strain alignment. MerF was weakly aligned in micelles by addition of Dy^{2+} to the solution NMR sample, as previously described.[30]

NMR Experiments. Solid-state NMR experiments were performed on aligned lipid bilayers with the bilayer normal parallel to the direction of the applied magnetic field. Hydrated slides were wrapped in plastic film, heat-sealed in polyethylene tubing, and placed inside the "flat-coil" of a probe double-tuned for the ^{1}H and ^{15}N resonance frequencies of 700 and 70 MHz. Experiments were performed on a home-built spectrometer with a mid-bore 700/62 magnet (Magnex Scientific, Oxford, UK). Unaveraged ^{1}H−^{15}N dipolar coupling frequencies were measured from two-dimensional PISEMA spectra.[33,38]

Solution NMR experiments were performed on a Bruker DRX 600 MHz spectrometer. ^{1}H−^{15}N residual dipolar couplings were measured using the IPAP−HSQC[39] experiment modified for the suppression of NH_2 signals from polyacrylamide.[40]

Calculations. The sinusoidal oscillations of ^{1}H−^{15}N dipolar couplings as a function of residue number are a direct consequence of the individual backbone NH bonds in an ideal α-helix being distributed on a cone and tilted at an angle δ (=15.8°) away from its long axis (Figure 1A). Indeed, information about the orientations of helices is manifested in the amplitudes, average values, and phases of the sinusoids that characterize the periodic oscillations of the dipolar couplings as a function of residue number.[1,2] The distribution of the θ and ϕ angles for each NH bond on this cone is described by the expression[2]:

$$D_{NH} = D_a\left\{(3\cos^2\theta - 1) + \frac{3}{2}R(1 - \cos^2\theta)\cos(2\phi)\right\} \qquad (1)$$

with $\cos\theta = \cos\theta_{av}\cos\delta - \sin\theta_{av}\sin\delta\cos(\rho - \rho_0)$ and $\phi = \phi_{av} + \sin^{-1}\{[\sin\delta\sin(\rho - \rho_0)]/\sqrt{1-\cos^2\theta}\}$. The fitting of this expression to simple sinusoids, which have been fitted to experimental measurements, yields information about the orientations of helices in the relevant frame of reference. In the case of completely aligned samples, the orientation of the *z*-axis of the alignment frame is parallel to the magnetic field

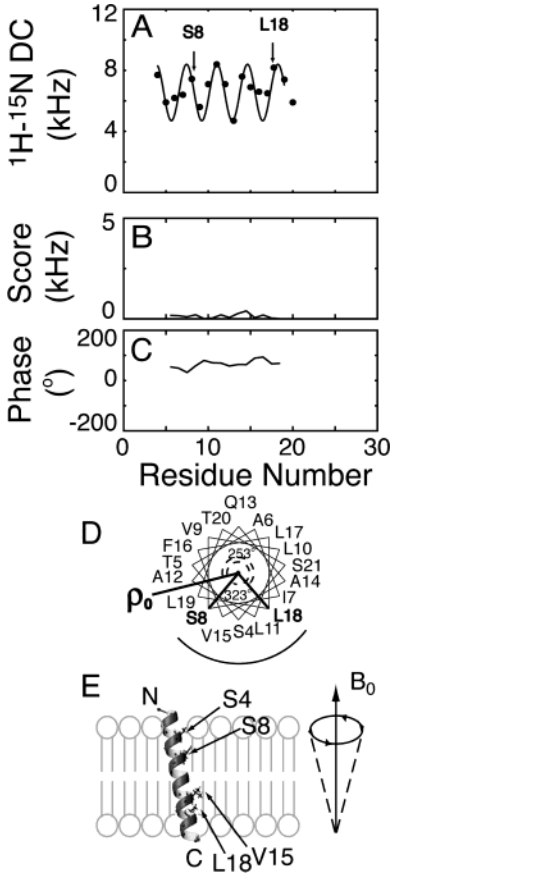

Figure 3. (A) Experimentally measured dipolar couplings for residues S4 through S21 in the membrane-embedded M2 peptide from the nicotinic acetylcholine receptor. Superimposed on the data are the best fitting sinusoid and the parametrized expression for the ^{1}H−^{15}N dipolar coupling as a function of residue number in an α-helix. The values for S8 and L18 are highlighted demonstrate the mapping of phase in a sine wave and position in a helical wheel. (B) The RMSD to an ideal sinusoid is measured for each window of four residues as less than 180 Hz. (C) Absolute phase of the best fitted sinusoid is constant, indicative of one continuous helix. (D) The helical wheel diagram shows the mapping of the pore-forming face of the helix and how the relative rotations of those residues map to the model shown in part E. The uniaxial distribution is shown as a cone with the 14° tilt angle.

direction, the magnitude is equal to that of the full static ^{1}H−^{15}N heteronuclear dipolar interaction, and the rhombicity contribution for a uniaxially aligned sample is zero. For weakly aligned samples, the magnitude and rhombicity of the alignment tensor are determined from the range of values observed in the experimental data. The magnitude and rhombicity of the alignment tensor can also be determined by best fitting eq 1 to the experimental data with all five variables (D_a, R, θ, ϕ, and ρ) allowed to vary in the fitting. This method is less robust, and it is common to find small variations from one helix to the next in the same polypeptide.

The identification of the residues in each helix was accomplished by nonlinear optimization of the fit of the phase and amplitude of a simple sinusoid of periodicity 3.6. A sliding window function of four or six residues was applied to the entire sequence. For the identification of helices, no information about the magnitude and rhombicity of the alignment is utilized. The amplitude, average value, and phase of the fitted sinusoids are not used directly at this stage of the process to determine the orientation of the helix. Contiguous residues are designated as constituting a helix when the average error per point for each window is less than or similar to the experimental error of the measurements, which we estimate to be 0.2 kHz for unaveraged dipolar couplings and 0.4 Hz for residual dipolar couplings.

(38) Wu, C. H.; Ramamoorthy, A.; Opella, S. J. *J. Magn. Reson.* **1999**, *140*, 131−140.
(39) Ottiger, M.; Delaglio, F.; Bax, A. *J. Magn. Reson.* **1998**, *131*, 373−378.
(40) Ishii, Y.; Markus, M. A.; Tycko, R. *J. Biomol. NMR* **2001**, *21*, 141−151.

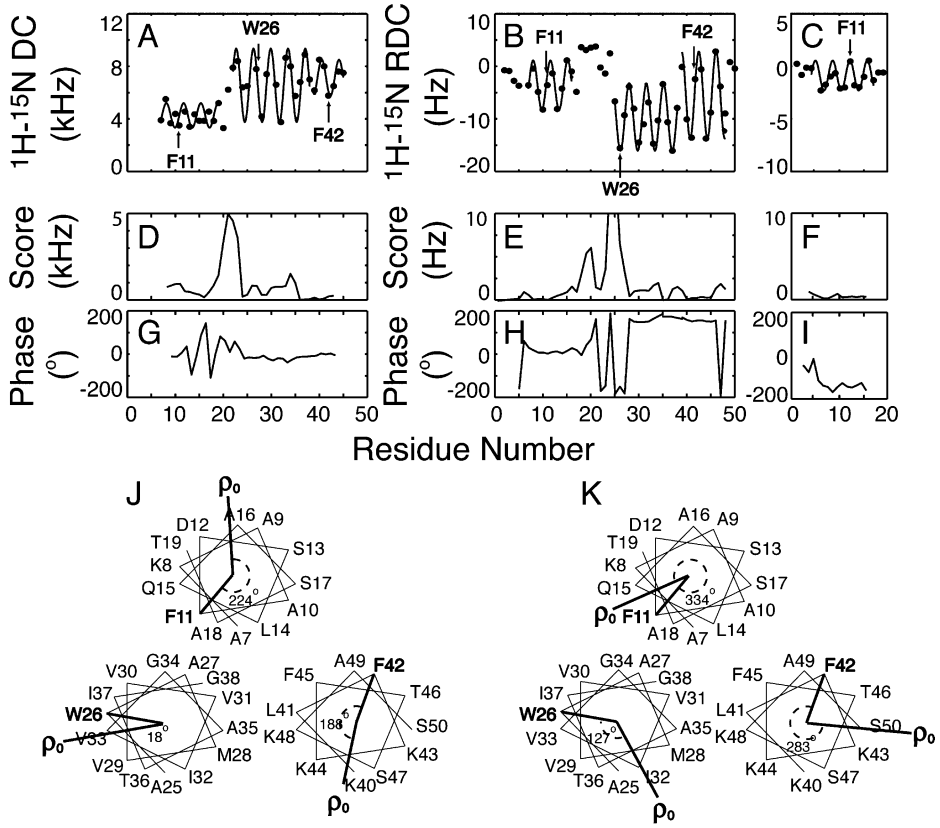

Figure 4. Experimentally measured dipolar couplings are shown for an (A) fd coat protein in completely aligned bilayers, (B) fd coat protein in weakly aligned micelles, and (C) fd^N (N-terminal 20 residues) in weakly aligned micelles. All datasets are shown with the best-fitting sinusoid and the parametrized expression yielding the tilts and rotations of the helices in the alignment frame. Shown below each dataset (D, E, F) are the RMSD to an ideal sinusoid and (G, H, I) the absolute phase of that sinusoid for each point. (J, K) Helical wheel diagrams show how the phase of the sinusoids maps to the periodicity of the helix. The residues F11, W26, and F42 are marked to show the rotation of the helices.

Values for the magnitude and rhombicity of the alignment tensor are then held fixed, and nonlinear least-squares fitting is used to determine the values of θ_{av}, ϕ_{av}, and ρ_0 that optimize the fit of the geometry of an ideal α-helix to the experimentally determined best-fitting sinusoid. The parametrized expression is written as a function of residue number n with $\rho - \rho_0 = (360°/3.6)n - \rho_0$; θ_{av} and ϕ_{av} are the spherical polar angles that describe the orientation of the helix axis in the frame of reference that describes the alignment of the protein in a frame which describes the orientation of the molecule. The rotation of a particular residue in a helix, ω_n, is given by the value of $(\rho - \rho_0)$ for that residue, thus defining the overall rotation of the helix in the alignment frame. Simple models of ideal α-helices ($\Phi = -62°$, $\Psi = -41°$) are rotated to their orientations using the screen *x*, *y*, and *z* axes as the axes of the alignment tensor, positioned using MOLMOL[41] so that the lengths of loops between helical segments correspond to 3.0 Å times the number of residues in that loop. Selected side chains are added to backbone structures as their most probable rotamer using the program SCWRL,[42] which enables the rotation angle of the helices to be visualized.

For data obtained from completely aligned bilayer samples, the uniaxial symmetry allows the unambiguous determinations of the tilt angle of the helix in the bilayer as well as the rotation angle about the long axis of the helix. For weakly aligned proteins, the dependence of the averaging on the azimuthal angle ϕ is taken into account, resulting in four possible orientations for a particular helix in the order frame. For each pair of values (θ_{av},ϕ_{av}) that determine the orientation of each helix in the alignment frame, $(\theta_{av},\phi_{av} + 180°)$, $(180° - \theta_{av}, 180° - \phi_{av})$, and $(180° - \theta_{av}, 360° - \phi_{av})$ are also possible. This results in 4^N possible models for *N* helices; however, since one out of each set of four is the same as one of each other set, the actual number of possibilities is reduced to 4^{N-1}. These ambiguities can be resolved by comparison to data obtained from a differently aligned sample.[43] For kinked helices or helices connected by short linkers, the number of possibilities are further limited by the covalent geometry of the molecule, and for clarity, this is considered as only one solution. It is also possible to identify the actual orientations of helices by reference to solid-state NMR data obtained on completely aligned samples.

To demonstrate the effects of deviations from ideal geometry on the appearance of dipolar waves simulated values for the unaveraged $^1H-^{15}N$ dipolar couplings are shown for typical deviations from ideality in Figure 2. In general, the periodicity is unaffected, while the changes in average value and amplitude reflect the change in orientation of the local helix axis. Curvature gradually changes these values, and kinks cause abrupt changes.

Results

The unaveraged dipolar couplings for all backbone amide sites of the uniformly ^{15}N labeled channel-forming M2 peptide plotted in Figure 3A were measured from a two-dimensional PISEMA spectrum obtained on a completely aligned bilayer sample.[35] The sinusoid that best fits those dipolar couplings that oscillate with a periodicity of 3.6 residues per turn is superimposed on the experimental data in Figure 3A. The quantitative results of the application of a four-residue sliding-window scoring function[2] to the M2 peptide data are shown in Figure 3B and C.

(41) Koradi, R.; Billeter, M.; Wuthrich, K. *J. Mol. Graphics* **1996**, *14*, 51−55.
(42) http://www.fccc.edu/research/labs/dunbrack/scwrl/. Dunbrack, R. L.; Cohen, F. E. *Protein Sci.* **1997**, *6*, 1661−1681.
(43) Al-Hashimi, H. M.; Prestegard, J. H. *J. Magn. Reson.* **2000**, *143*, 402−406.

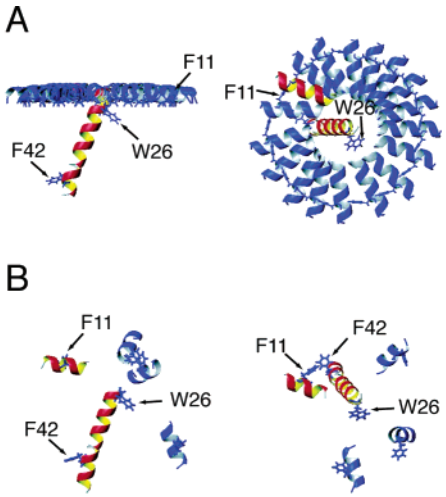

Figure 5. Models of the fd coat protein helices consistent with the dipolar wave results in Figure 2. (A) The uniaxial symmetry of the unaveraged dipolar couplings gives a conelike distribution of possible orientations for one helix relative to the other but fixes the orientation relative to the lipid bilayer. (B) The inherent degeneracy of RDC measurements leads to four possible models of the coat protein. The models shown here are drawn for an arbitrary alignment. Residues F11, W26, and F42 are highlighted to show the rotations of the helices about their long axes. The models most consistent with the full structure characterization of this protein are shown in red.

They show that the experimental dipolar coupling data oscillate with a periodicity of 3.6 between residues S4 through S21 but not for the C- and N-terminal residues. The average error per measurement for the sinusoid shown in Figure 3A for residues S4 through S21 is 160 Hz, which is less than the experimental error. Not only does the sinusoid fit the periodic oscillations of the data extremely well but also it has constant phase, as shown in Figure 3C. Taken together, the parameters in Figure 3 demonstrate that residues S4 through S21 form a nearly ideal α-helix that crosses the bilayer with a tilt angle of 14°.

In addition, the positions of the experimental data points on the dipolar wave reflect the rotation of the helix in the bilayer. The side chains of the pore-lining residues S4, S8, V15, and L18[44] are highlighted in Figure 3D in the context of a helical wheel diagram.[45] The position of ρ_0 determined from the fit and parametrization reflects the position in the helix that is tilted farthest away from the alignment *z*-axis. The rotations of residues S4 and L18 can be determined from their position along the sinusoid with values of 323° and 253° for S8 and L18, respectively. Because the polypeptide is immobile and completely aligned in the bilayer sample, the global orientation and the tilt and rotation of the helix are determined by the properties of the dipolar wave and are illustrated in Figure 3E. The dipolar wave indicates that the helix is straight, has a tilt of 14°, and has the rotation shown in Figure 3E, all in agreement with the previously determined three-dimensional structure.[35]

The 50-residue fd coat protein is a typical membrane protein with a long hydrophobic transmembrane helix and a shorter amphipathic in-plane helix connected by a turn or loop,[26,46] and it has mobile C- and N-terminal residues. The secondary structures and relative orientations of the helices in the membrane-bound form of the fd coat protein can be directly

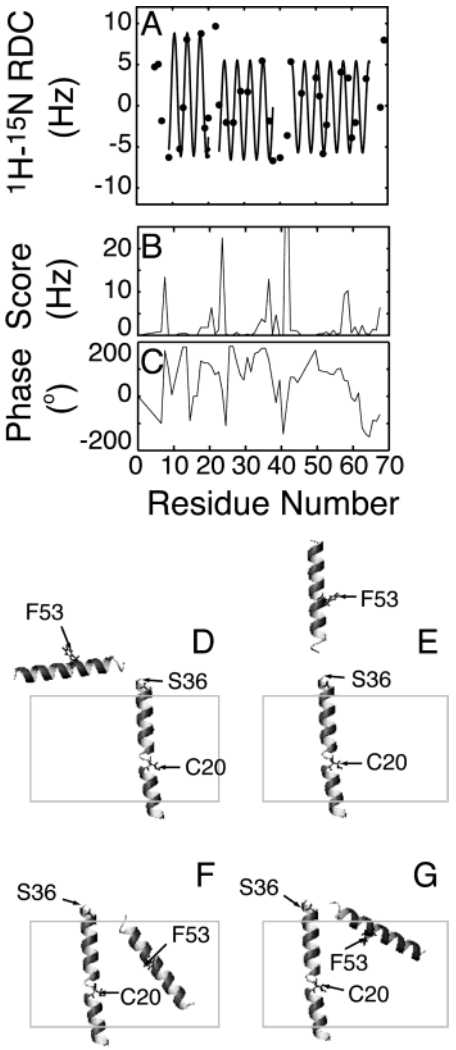

Figure 6. (A) Experimental $^1H-^{15}N$ residual dipolar couplings measured for MerF in weakly aligned micelles. (B) The periodicity, despite some missing measurements (designated by dotted lines), is indicative of three helical segments, with a change in direction near the middle of the first helix. (C) The absolute phase of the fitted sinusoid gives an idea of the continuity of the periodicity. Four possible models of the protein are shown in D, E, F, and G. Model F is most consistent with experimental data obtained from solid-state NMR. The positions of residues C20, S36, and F53 are shown.

determined from the experimental data and fits to sinusoids shown in Figure 4. The results of three experiments on two different polypeptides, the full-length fd coat protein and the 20-residue fd^N peptide that corresponds to the N-terminal amphipathic helix of the coat protein, are analyzed in the figure. The dipolar couplings in Figure 4A were measured on a sample of the coat protein in completely aligned bilayers, while the residual dipolar couplings in Figure 4B and C were measured from samples of the 50-residue and 20-residue polypeptides, respectively, in weakly aligned micelles. The protein has very similar properties in bilayer and micelle environments. For example, using the periodicity of the oscillations of the dipolar couplings as a strict criterion, the number of residues in the N-terminal amphipathic helix is well defined and nearly identical in all three samples. Similarly, the length and other properties of the hydrophobic helix in the full-length protein are the same in micelles and bilayers. The average error per measurement for the fit of a four-residue sliding window function is shown

(44) (a) Oiki, S.; Madison, V.; Montal, M. *Proteins* **1990**, *8*, 226−236. (b) Akabas, M. H.; Kaufmann, C.; Archdeacon, P.; Karlin, A. *Neuron* **1994**, *13*, 919−927.
(45) Schiffer, M.; Edmundson, A. B. *Biophys. J.* **1967**, *7*, 121−135.
(46) Marassi, F. M.; Opella, S. J. *Protein Sci.* **2003**, *12*, 403−411.

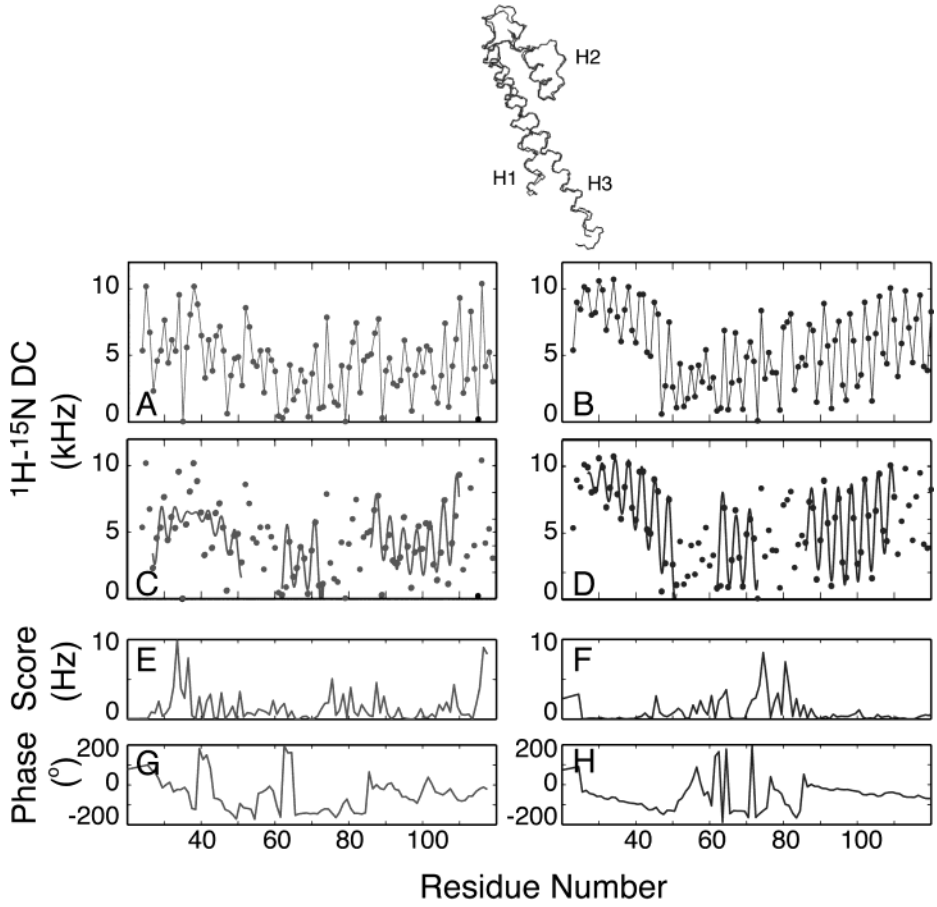

Figure 7. (A and B) Simulated $^1H-^{15}N$ dipolar couplings for the previously determined structures KcsA with RMSDs of 3.2 Å[13] and 2.0 Å.[14] Simulations are performed using the FORTRAN program SIMSPEC, which takes as input the coordinates from the PDB files (protons added using MOLMOL) for the alignment shown at the top, where the protein is completely uniaxially aligned. (C and D) The same data with the best fitting sinusoids of a periodicity of 3.6 superimposed on the data. Parts E and G show that the scoring functions for a periodicity of 3.6 residues in the case of the 3.2 Å structure are not able to determine the locations of the two long helices. Parts F and H are more typical of well-fitted sinusoids showing that the score is low along all three helices and the phase is nearly constant as well.

in Figure 4D, E, and F, and the absolute phases for each window are shown in Figure 4G, H, and I. The large increase in the score between residues Q15 and I22 in Figure 4D and E is evidence of the lack of periodicity in the structures of the residues in the loop connecting the two helices. The helices are straight within experimental error, as evidenced by the low fitting errors for each helix. The average error per residue is 200 Hz for the solid-state NMR data shown in Figure 4A and 0.4 Hz for the solution NMR data for each helix in Figure 4B and C.

The amphipathic α-helix begins at A7 (which follows P6) and ends at T19 in bilayers and S17 in micelles. There are few discernible differences in the N-terminal helix due to the presence of the hydrophobic helix, demonstrating that the two helices are independent structural entities. In addition, there are no noticeable differences in the properties of this helix in micelle and bilayer samples, indicating that this helix is not affected by the curvature or another property of the lipid assembly. This differs from a recent result on a different, longer polypeptide compared in micelle and bicelle samples.[47] The positions of residues F11, W26, and F42 are used as markers to characterize the rotations of the helices in the context of helical wheel diagrams (Figure 4J, K, L). The tilt angles and rotations of the α-helices determined in their alignment frames by dipolar waves are used to generate the models of the fd coat protein in bilayers shown in Figure 5A and in micelles in Figure 5B, which illustrate the orientational ambiguities in these data. The solid-state NMR data on an aligned bilayer sample give the absolute orientation of the amphipathic helix with the uniaxial distribution of possibilities shown. The four possible relative orientations of the amphipathic helix are also shown in Figure 5. These types of ambiguities can generally be resolved for membrane proteins through additional data, comparisons of solid-state NMR and solution NMR data, and structural restraints where there are only a few residues separating helical segments.

A detail of the membrane-bound form of the coat protein structure that may have significance when it is assembled into bacteriophage particles is the change in helix direction after residue G38. Remarkably, this same kink is found in the membrane-bound form of the protein, in both micelles (Figure 4A) and bilayers (Figure 4B), and in the structural form of the protein that interacts with DNA but not lipids in the coat of the bacteriophage particles.[48] This kink is evident from the rise in the score for that region of the helix in Figure 4D and less dramatically in Figure 4E. The irregular patterns of the dipolar couplings of the residues connecting the amphipathic and

(47) Chou, J. J.; Kaufman, J. D.; Stahl, S. J.; Wingfield, P. T.; Bax, A. *J. Am. Chem. Soc.* **2002**, *124*, 2450−2451.

(48) Zeri, A. C.; Mesleh, M. F.; Nevzorov, A. A.; Opella, S. J. *Proc. Natl. Acad. Sci. U.S.A.* **2003**, *26*, 327−334.

hydrophobic helices demonstrate that there are substantial differences between the short bend in bilayers and the larger, more complex loop structure in micelles. There is evidence from relaxation data that these residues have internal mobility in the micelle samples.[26] In bilayers, the trans-membrane helix begins at residue Y21, while in micelles this helix begins at W26. This points to the importance of paying particular attention to residues near the bilayer interface in structural studies of membrane proteins. In general, the small size of the interhelical loops in bilayer samples restricts the possible relative orientations of the two helices, thereby limiting the ambiguities in helix orientations.[46]

MerF is an 80-residue (as expressed) mercuric ion transporter associated with the bacterial mercury detoxification system found in bacteria that display resistance to toxic levels of Hg^{2+} ions.[49] The dipolar waves fitted to the RDCs measured from experiments on weakly aligned MerF in micelles are shown in Figure 6A. Most models for this protein based on hydropathy plots and genetic data have two transmembrane helices. However, the scoring parameters shown in Figure 6B, C indicate that there are two major breaks in the 3.6 residue per turn periodicity, near residue C21 and near residue G40. The smaller apparent increase in score near A38 reflects two missing RDC measurements. The helix orientations obtained from these fits and shown in Figure 6D are consistent with the break at C20 arising from a kink and the four residues between L38 to L42 constituting a loop between the two hydrophobic helices. Significantly, C20 and C21 are essential for the Hg^{2+}-binding function of the protein; therefore, a break in the helix at this position is compatible with their ability to bind and transport Hg^{2+} ions across the cell membrane. Four symmetry-related models are consistent with the NMR data. Taking into account the high hydrophobicity of the residues in the first helix leads to the selection of the model that is most realistic (F). This is also the model that is in accord with solid-state NMR measurements on bilayer samples. It is interesting to note that this model places F53 beside the functional C20, a detail that this protein has in common with MerP,[50] its periplasmic Hg^{2+} binding partner. This is in keeping with the high level of conservation of this phenylalanine in MerF and a number of related proteins. Thus, the structural information derived from dipolar waves can lead to plausible speculation about the roles of specific residues in the function of a membrane protein.

Discussion

Dipolar waves are sensitive indicators of the structures, orientations, and rotations of helices in proteins; therefore, they are well suited for the characterization of helical membrane proteins. The high quality of the fits of the experimental data in Figures 2, 3, and 6 to ideal sinusoids is consistent with little or no deviation from the structure of an ideal α-helix. Indeed, abrupt changes in score or phase are diagnostic of kinks. Curvature of helices can also be detected through the use of dipolar waves.

The sensitivity of dipolar waves to deviations from ideality of helices in membrane proteins is demonstrated in Figure 7A and B using dipolar coupling data simulated from the structure of the bacterial potassium channel KcsA determined at two different levels of resolution.[13,14] It can be seen from simulations

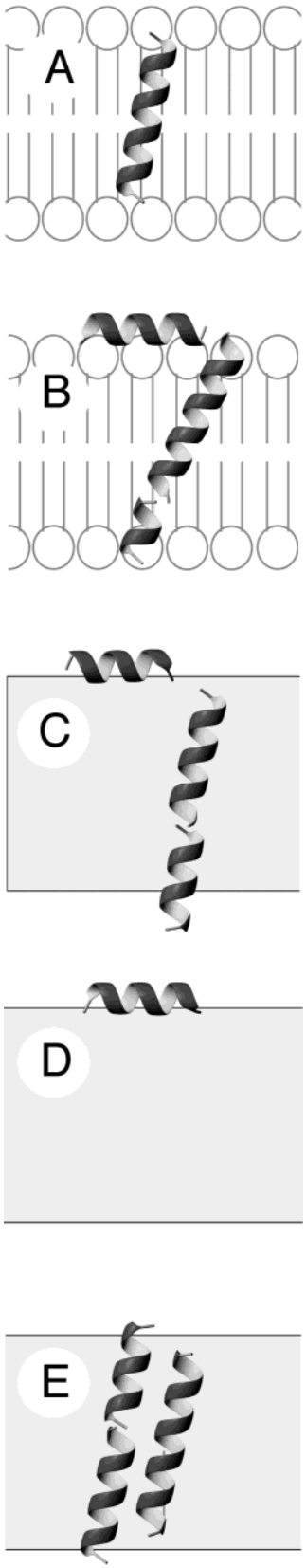

Figure 8. Helices in membrane proteins. (A) M2 peptide in bilayers. (B) The fd coat protein in bilayers. (C) The fd coat protein in micelles. (D) N-terminal peptide of the fd coat protein in micelles. (E) MerF protein in micelles.

(49) Wilson, J. R.; Leang, C.; Morby, A. P.; Hobman, J. L.; Brown, N. L. *FEBS Lett.* **2000**, *472*, 78−82.
(50) Steele, R. A.; Opella, S. J. *Biochemistry* **1997**, 36, 6885−6895.

of the unaveraged $^{1}H-^{15}N$ dipolar couplings that while the helical structure can be identified in the 3.2 Å resolution structure, the irregularity of this structure is sufficient to affect the appearance of the dipolar waves, and the periodicity of the two long helices is difficult to discern. Only helix 2 shows clear periodicity in the scores in Figure 7E, G. In contrast, dipolar couplings simulated from the 2 Å resolution structure show unmistakable periodicity. The scoring in Figure 7F, H identifies all three helices and clearly defines their boundaries. Moreover, the decrease in the magnitudes of the dipolar couplings along the sequence is evidence of the curvature of helix 1. The long helix 3 also shows some evidence of curvature but less than that for the first helix. The backbone RMSD between the two crystal structures is only 0.7 Å, yet there are dramatic differences in the oscillatory behavior that demonstrate the sensitivity of dipolar waves to structural details. Only in the higher resolution example can tilt angles and rotations of these helices be reliably extracted from fits to the dipolar couplings. This example demonstrates that when the experimental NMR data show analyzable periodic oscillations, such as the data in Figures 3, 4, and 6, then the structural analysis with dipolar waves yields results that have a resolution equivalent to RMSDs less than 2 Å. Thus, dipolar waves have the potential to provide atomic resolution structures of large portions of the backbones of membrane proteins.

The structural features of the membrane peptides and proteins analyzed with dipolar waves are compared in the context of lipid bilayers in Figure 8. The helix orientations shown in Figure 8 parts A and B are determined from experiments performed on completely aligned lipid bilayer samples; therefore, they reflect the global orientation of the protein in the bilayer. The helix orientations shown in Figure 8 parts C, D, and E are based on results from weakly aligned micelle samples. Therefore, the relative orientations of helices in the same polypeptide are based on dipolar waves, but the global orientations reflect comparisons with solid-state NMR data. Figure 8 parts B and C compare the structures of the fd coat protein in bilayer and micelle environments, while that in Figure 8D extends the comparison to the effects of truncation of the protein on the structure and orientation of the N-terminal amphipathic helix.

The conformations of 63%−72% of all residues in the examples of small helical membrane proteins shown in Figure 8 are characterized with atomic resolution by dipolar waves. Since there are generally several mobile residues at the termini and in interhelical loops of small helical membrane proteins, dipolar waves may be able to describe as many as 80% of the structured residues in this class of proteins. Therefore, they have the potential to provide a straightforward method for determining major portions of the three-dimensional structures of membrane proteins with multiple helices. Further, the experiments can be performed in ways[46,51] that lead to the high throughput needed for characterization of a large fraction of proteomes that are helical membrane proteins.

Acknowledgment. We thank D. H. Jones and A. Nevzorov for helpful discussions. This research was supported by Grants R37GM24266, P01GM64676, R01GM29754, and R01CA82864 from the National Institutes of Health and utilized the Biomedical Technology Resource for Solid-State NMR of Proteins, supported by Grant P41RR09731. D.S.T. was supported by Postdoctoral Fellowship F32GM63300 from the National Institutes of Health.

JA034211Q

(51) Lee, S.; Mesleh, M. F.; Opella, S. J. *J. Biomol NMR* **2003**, *26*, 327−334.